Desalination and Water Treatment
www.deswater.com

doi: 10.5004/dwt.2017.21032

81 (2017) 152–161
June

Removal of fluoride from aqueous solution using Amberlite-IRA-aluminum sorbent nanoexchanger

Mostafa M. Emara[a,b], Aida A. Salman[a,c], Nesrine M. R. Mahmoud[d,e,*], Samah A. Fattah[a,c]

[a]*Science Center for Detection and Remediation of Environmental Hazards, Al-Azhar University, Cairo, Egypt*
[b]*Faculty of Science (Boys), Al-Azhar University, Cairo, Egypt, email: scdreh@yahoo.com*
[c]*Faculty of Science (Girls), Al-Azhar University, Cairo, Egypt, emails: a_mnaser@hotmail.com (A.A. Salman), samahabdlfattah2013@yahoo.com (S.A. Fattah)*
[d]*Faculty of Pharmacy, Nahda University (NUB), Egypt*
[e]*Basic Science Department, Preparatory Year Deanship, University of Dammam, Saudi Arabia, email: nmmahmoud@uod.edu.sa*

Received 7 December 2016; Accepted 12 June 2017

ABSTRACT

In the present study, aluminum-modified anionic exchanger nanoparticles were synthesized by introducing Al(III) ions onto the functional sites of the polymeric anion exchanger Amberlite-402. The modified anionic exchanger gathered the favorable sorption properties of inorganic nanoparticles with the excellent hydraulic characteristics of polymeric beads. Hazardous persistent fluoride ions in water were removed by the new sorbent using both batch and fixed-bed column techniques. Different parameters that affect the adsorption process such as initial concentration, pH, and temperature have been investigated. It is found that the adsorption of fluoride ions is efficient in a wide range of pH. However, maximum removal is observed at pH = 3.0. In addition, the adsorption capacity is slightly affected by temperature and is increased by decreasing the temperature from 308 to 288 K to reach 80.33 mg g^{-1}. The coexisting ions chloride and nitrate were also studied. Their existence had a significant effect on reducing the efficiency of fluoride removal from 24.5 to 17.5 mg g^{-1} and 15.0 mg g^{-1}, respectively. The study showed that the adsorption process favored the Langmuir adsorption model. Thermodynamic parameters were also calculated and positive $\Delta G°$ values were related to a non-spontaneous nature of the adsorption. Fixed-bed column experiments were carried out for investigating the following parameters: influent fluoride concentrations, bed depths, and various flow rates. The breakthrough time increased either with increasing flow rate, decreasing bed depth, or decreasing influent fluoride concentration. The X-ray diffraction, energy dispersive X-ray spectroscopy, and scanning electron microscope studies were carried out for the characterization of the new sorbent. These studies confirmed that aluminum ions are successfully loaded onto the surface of Amberlite-402. This study proves that novel Amberlite-IRA-Al is more efficient than other defluoridation techniques.

Keywords: Ion-exchange; Fluoride; Aluminum sorbent; Adsorption; Regeneration

1. Introduction

Fluoride is one of the persistent, non-biodegradable, and hazardous pollutants that accumulate in wildlife and human [1]. According to the World Health Organization, the maximum acceptable concentration of fluoride ions in drinking water lies below 1.5 mg g^{-1} [1]. Fluoride, at low concentrations, has beneficial effects on health, however, with increasing fluoride concentrations, the number of adverse effects on health increased. These hazardous effects

* Corresponding author.

of fluoride ranged from mild to crippling fluorosis depending on the period and level of exposure. In the mild version of fluorosis, teeth become mottled, however, in the highest one, bones become embrittle [1,2]. Some studies have shown that there is a relation between fluoride toxicity and kidney diseases. Excessive intake of fluoride can give rise to various diseases like osteoporosis, arthritis, cancer, brittle bones, infertility, Alzheimer syndrome, brain damage, and thyroid disorder [1]. The risk of fluorosis and other diseases associated with consumption of water with high fluoride concentration is a serious problem in some countries [1]. Many conventional methods are applied for fluoride removal from water as liming accompanied by precipitation [1,3]. Other methods include ion-exchange [1,4], activated alumina [5], and electrocoagulation [6,7]. The usage of these methods is limited by various unfavorable factors like high cost of operation and maintenance, generation of toxic by-products [1].

"A number of nanoscale inorganic particles (NIPs) offer favorable properties in regard to selective separation and/or chemical transformation of target contaminants." Preparation of these particles and their aggregation is operationally simple, environmentally safe, and inexpensive. These particles offer very favorable kinetics for oxidation–reduction and selective sorption reactions due to their high surface area to volume ratio. However, due to poor durability and excessive pressure drops, we cannot use these particles in fixed-bed columns [8–10]. In contrast, the polymeric beads are very durable, commercially available, and offer excellent hydraulic properties. So, it would be considered necessary to develop new materials that gather the favorable sorption properties of inorganic nanoparticles with the excellent hydraulic characteristics of polymeric beads [8]. There also exists an effective and popular chemical material used in fluoride removal which is the activated alumina; it is difficult to be widely used due to its high cost. Hence, recent studies focused on the research of modified methods have been recommended. Due to the high electrical affinity for fluoride ion, some rare earth elements and metal ions such as La^{3+} [11–13], Ce^{3+} [14], Al^{3+} [15], and Fe^{2+} [16] are used to improve the fluoride adsorption capacity of modified adsorbents. These kinds of ions loaded onto natural materials appeared more appropriate and seductive in various chemical modifications.

The broad objective of this study is to modify the capacity of a certain type of anionic exchanger with aluminum nanoparticles and to explore the feasibility of this new sorbent for the removal of fluoride ions from aqueous solution using batch and column techniques. In this study, we will investigate different parameters related to batch technique as initial concentration, pH, and temperature. In addition to performing column studies to investigate the fluoride uptake characteristics of Amberlite-IRA-Al under different flow rates, bed depth, and concentration.

2. Experimental

2.1. Materials

Amberlite-402-Cl was purchased from Rohm and Haas (Philadelphia, USA). Other chemicals used throughout the experiments were analytical grade otherwise specified. All required concentrations of fluoride were prepared by diluting the stock solution of 1,000 mg L^{-1}. Deionized water was used for the preparation of all solutions.

2.2. Synthesis of the new sorbent

Amberlite-402-Cl is a premium grade strong basic anion exchange resin with a clear gel structure. It is based on cross-linked polystyrene and has very high bead integrity. The preparation of the new polymeric/inorganic sorbent includes the following three steps [17,18].

Step 1: Loading of Al(III) onto the functional sites of the anion exchanger by passing 4% $AlCl_3$ solution.
Step 2: Desorption of Al(III) and simultaneous precipitation of Al(III) hydroxides within the gel and pore phase of the exchanger through the passage of a solution containing both NaCl and NaOH, each at 5% w/v concentration.
Step 3: Rinsing and washing with a 50/50 ethanol–water solution followed by a mild thermal treatment (50°C–60°C) for 60 min.

2.3. Batch experiments

All batch equilibrium experiments were conducted in a 250 mL polyethylene bottle, by contacting 0.1 g sorbent with 100 mL of fluoride solution at different influent initial concentrations and pHs. The samples were shaken for 60 min using Shaker Bath (Stuart Scientific) SBS 30. The concentration of fluoride ions was determined spectrophotometrically at 570 nm using SPADNS reagent [19,20].

2.4. Fixed-bed column experiments

Fixed-bed column runs were carried out using a constructed system, which consists of a glass column (11 mm in diameter) and a small (in–out) constant flow water pump connected to a power supply of 9 V. The flow rate for all runs was adjusted to be 2 mL min^{-1}. The flow rate remained practically constant during the whole experimental time. 5 mL aliquot from the effluent was analyzed regularly by the suitable technique till the breakthrough is reached [17,21,22].

3. Results and discussion

In the present study, aluminum-modified anion exchanger was used for the removal of fluoride ions from aqueous solution. The maximum adsorption capacity was found to be 80.33 mg g^{-1}; from equilibrium experiments at 288 K with sorbent dosage of 0.1 g. The aluminum-modified exchanger is characterized by scanning electron microscopy (SEM), energy dispersive X-ray spectroscopy (EDX), and X-ray diffraction (XRD). The effects of various influencing parameters such as the initial fluoride concentration, contact time, sorbent dosage, and pH are studied. The adsorption capacity of modified exchanger is compared with various adsorbents reported in the literature [1,23]. The adsorption capacity of aluminum-modified exchanger is found to be higher than many commercially available and low-cost adsorbents [24,25]. In the present work, the nanoporous sorbent was prepared in gel form, which makes it more applicable for continuous treatment of industrial effluent streams. The results of this study indicate that the prepared aluminum-modified

exchanger proves to be an efficient and effective sorbent that can be used for defluoridation of wastewater.

3.1. X-ray diffraction

The data obtained from X-ray diffraction Fig. 1, indicated that the Amberlite-IRA-Al sorbent possesses an amorphous structure due to the absence of any diffraction line which is characteristic of the crystalline phase, this may be due to that of the formed $Al(OH)_3$ particles are smaller than the detection limit of the instrument and located in the nano range which cannot be detected by XRD.

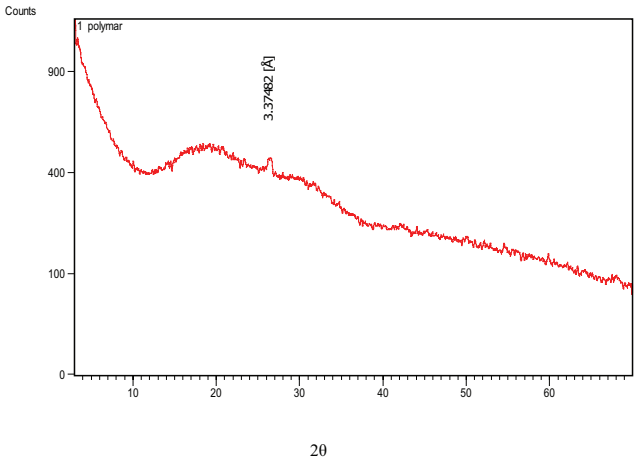

Fig. 1. XRD pattern of Amberlite-IRA-Al sorbent.

3.2. SEM and EDX characterization

The scanning electron microscope (SEM) images for Amberlite-IRA-Al sorbent Figs. 2(a)–(d) showed that the modification does not change the surface structure of raw Amberlite-402 and also showed that the surface was homogenous and no cracks formed on it. It was also observed that the aluminum particles were formed in the nanoscale ranged from 22.48 to 95.39 nm. The EDX spectra Fig. 3, an aluminum peak around 1.5 eV confirms the presence of aluminum ions onto the surface of Amberlite-402.

3.3. Parameters affecting removal capacity

3.3.1. Effect of pH

The effect of initial solution pH on fluoride removal by Amberlite-IRA-Al is shown in Fig. 4. The adsorption capacity was studied at pH in the range from 3.0 to 9.0 with an initial concentration of 25 mg L^{-1}. The adsorption

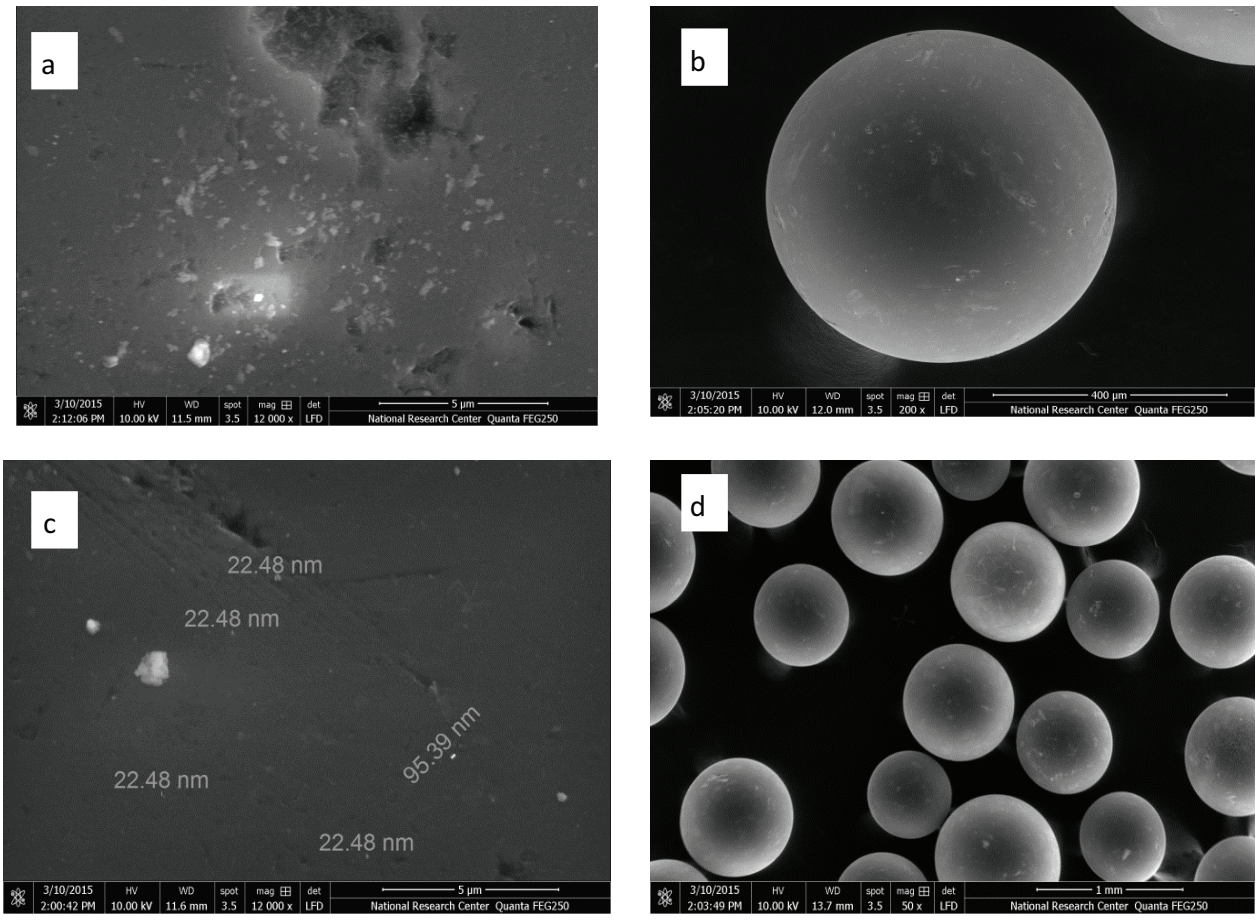

Fig. 2. SEM micrograph for (a) Amberlite-IRA-Al sorbent at magnification 12,000×, (b) the size of aluminum particles agglomerates, (c) Amberlite-IRA-Al sorbent at magnification 200×, and (d) Amberlite-IRA-Al sorbent at magnification 50×.

of fluoride ions is increased with pH decreasing from 9.0 to 3.0. Similar behavior has also been reported for the removal of fluoride in the literature [26]. The results indicated the high dependence on pH change and extensive adsorption capacity occurred at pH in the range of 3.0–7.0. This pH dependence is consistent with similar results obtained by MEDUSA software [27].

3.3.2. Effect of temperature

Fig. 5 shows the effect of temperature on fluoride removal by Amberlite-IRA-Al. It is elucidated from Fig. 5 that the adsorption capacity decreased by increasing the temperature from 288 to 308 K. The maximum removal of fluoride was observed at 288 K which is consistent with the previous comprehensive studies [25,28]. The calculated adsorption capacity of Amberlite-IRA-Al sorbent as 80.33 mg g^{-1} is a considerably high value compared with many adsorbents used to remove fluoride ion from water (Table 1) [29].

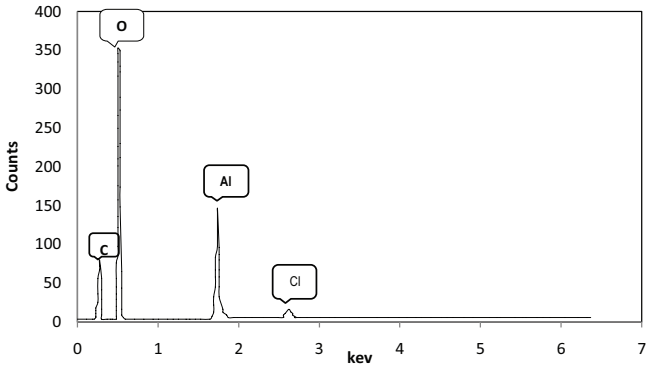

Fig. 3. EDAX spectra for Amberlite-IRA-Al sorbent show the presence of aluminum as an element.

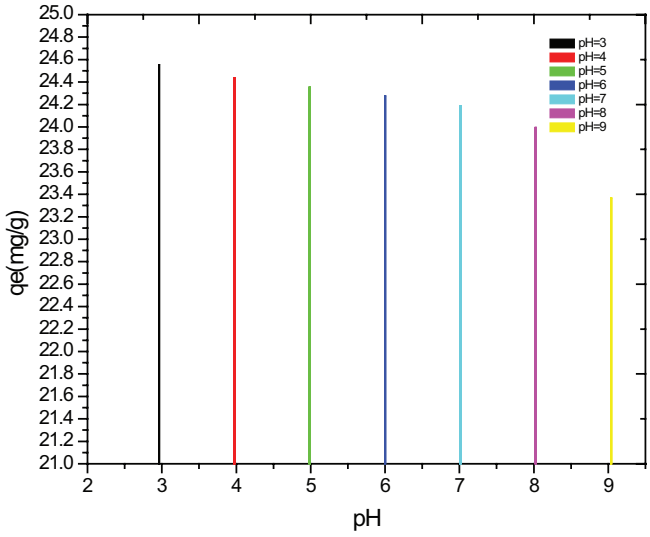

Fig. 4. The sorption capacity was studied at pH range from 3.0 to 9.0 with initial concentration of 25 mg L^{-1}.

3.3.3. Effect of contact time

The relationship between contact time and adsorption capacity was also studied. The fluoride uptake was very fast at the beginning accomplished almost after 8 min after which no significant change in adsorption was observed as illustrated in Fig. 6.

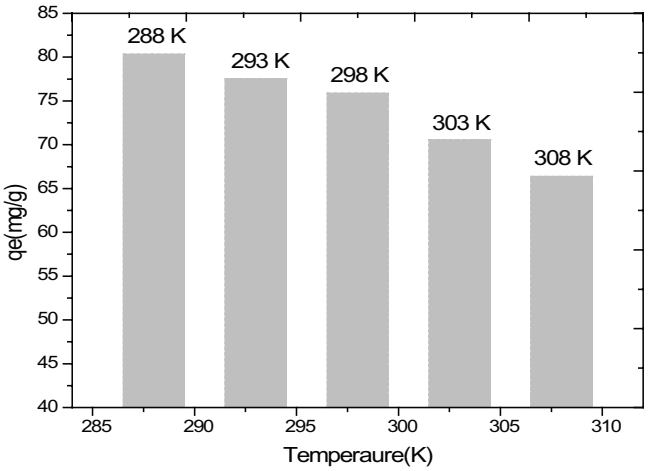

Fig. 5. Adsorption capacity of Amberlite-IRA-Al at different temperatures.

Table 1
Calculated constants of Langmuir isotherm

Temperature, °C	q_{max}, mg g^{-1}	K_L, L mg^{-1}	R^2
15	80.33	0.01263	0.99931
20	77.55	0.01315	0.99914
25	75.89	0.01380	0.99997
30	70.57	0.01433	0.99968
35	66.38	0.01514	0.99987

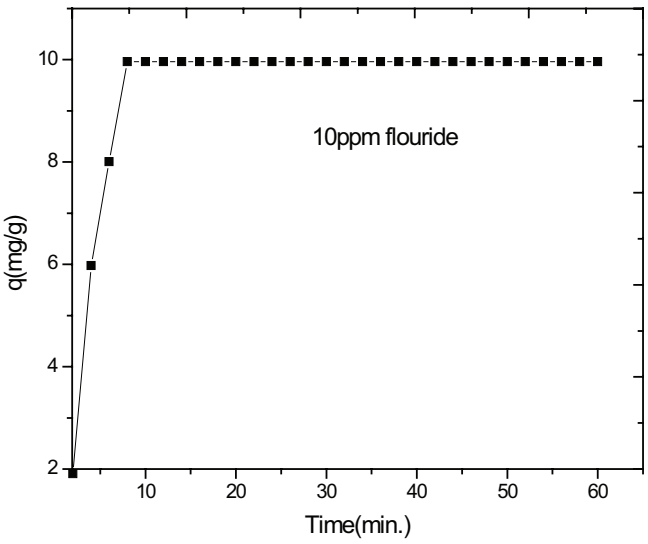

Fig. 6. Time vs. adsorption capacity of fluoride with initial concentration of 10 mg L^{-1}.

3.4. Adsorption isotherm model studies

To determine the adsorption efficiency, it is important to study adsorption isotherm.

One of the famous adsorption isotherms is Langmuir model which is applied in this study. The Langmuir adsorption isotherm assumes that the adsorption occurs on the homogeneous surface of the adsorbent material [30,31]. It also assumes that a monomolecular layer formed when adsorption takes place without any interaction between the adsorbed molecules [32]. The Langmuir (1916) linearized equation is represented as follows:

$$\frac{c_e}{q_e} = \frac{1}{q_m b} + \frac{c_e}{q_m} \quad (1)$$

where C_e is the equilibrium concentration mg L^{-1}, q_e is the amount of fluoride ions adsorbed at equilibrium mg g^{-1}, b the sorption equilibrium constant L mg^{-1}, and q_m the maximum saturation capacity of Amberlite-IRA-Al sorbent mg g^{-1} [33]. Plotting C_e/q_e vs. C_e and q_e vs. C_e illustrated in Figs. 7(a) and (b), respectively, proves the applicability of Langmuir model [32].

3.5. Adsorption kinetic studies

In this study, kinetic experiments were performed by placing 0.1 g sorbent into 250 mL bottles containing 10 mL of fluoride solution (25, 50, 75, and 100 mg L^{-1}) at 298 K and 250 rpm shaking speed for an hour. At suitable time intervals, 5 mL of the sample was withdrawn and the amount of fluoride was determined spectrophotometrically at 570 nm using SPADNS reagent. Pseudo-first-order and pseudo-second-order kinetic models were used to illustrate kinetics. The experimental data fitted pseudo-second-order according to the following equation which represents the linear form of this kinetic model [32].

$$\frac{t}{q_t} = \frac{1}{K_2 q_e^2} + \frac{t}{q_e} \quad (2)$$

In Fig. 8, plotting t/q_t vs. time indicated that the adsorption of fluoride onto Amberlite-IRA-Al sorbent fits better as a pseudo-second-order (R^2 = 0.999). Similar results were reported for adsorption of fluoride on aluminum alginate beads [28].

3.6. Thermodynamics studies

Thermodynamic parameters of an adsorption process are necessary to give clear explanation whether the process is spontaneous or not. The experimental data obtained at different temperatures were used in calculating the thermodynamic parameters such as Gibbs free energy change ($\Delta G°$), enthalpy change ($\Delta H°$), and entropy change ($\Delta S°$) [34]. The free energy change of the adsorption can be given as:

$$\Delta G° = -RT\ln K_L \quad (3)$$

where $\Delta G°$ is the Gibbs free energy of sorption kJ mol^{-1}, R is the gas constant (8.314 J mol^{-1} K^{-1}), and K_L is the Langmuir constant

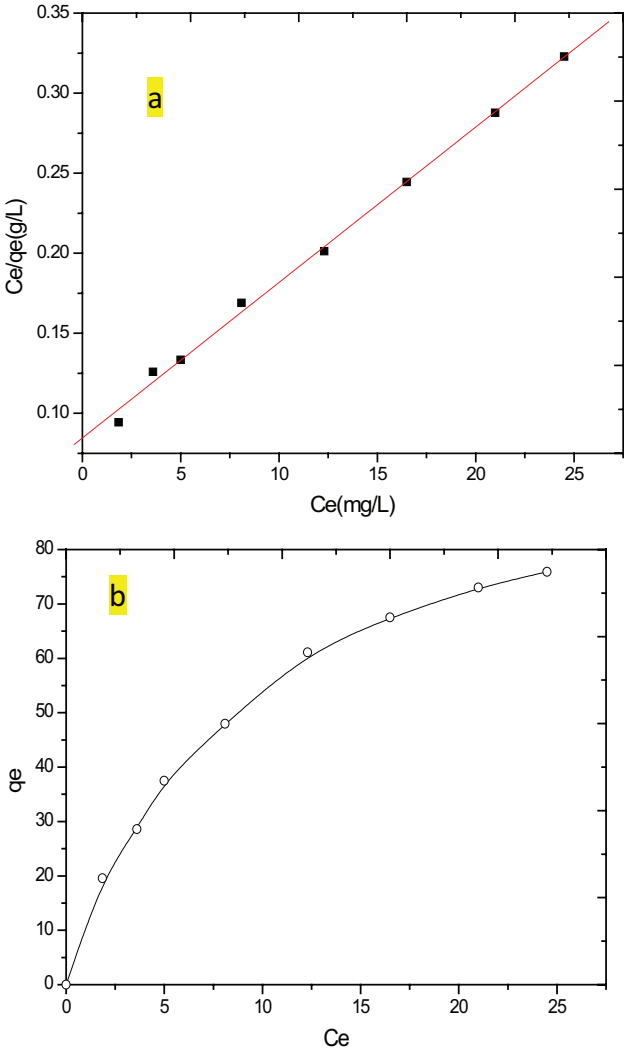

Fig. 7. (a) Langmuir isotherm for fluoride adsorption using linearized equation. (b) Langmuir isotherm for fluoride adsorption.

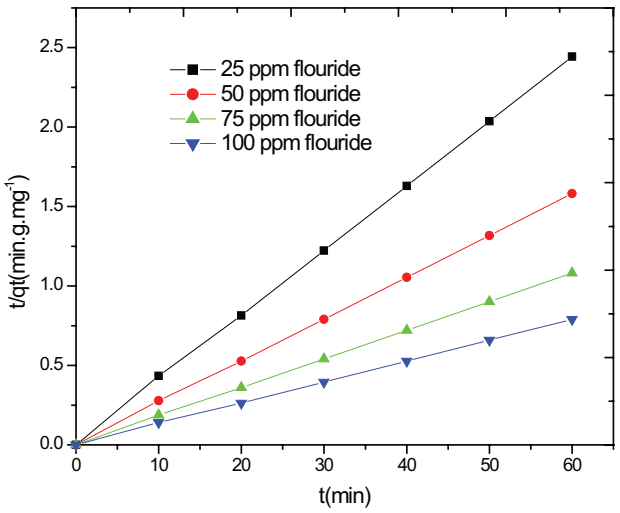

Fig. 8. Pseudo-second-order for removal of fluoride using Amberlite-IRA-Al sorbent.

for sorption. Positive D$G°$ values indicated non-spontaneous nature of the adsorption of F^- on Amberlite-IRA-Al (Table 2).

$\Delta H°$ and $\Delta S°$ were obtained from the slope and intercept of the linear variation of ln$K$ with 1/T. The thermodynamic parameters $\Delta G°$, $\Delta H°$, and $\Delta S°$ are calculated according to the van't Hoff equation [35]:

$$\ln K = \frac{-\Delta H}{R}\left(\frac{1}{T}\right) + \frac{\Delta S}{R} \quad (4)$$

The standard enthalpy and entropy changes of adsorption were determined to be 6.761 kJ mol^{-1} and –12.872 J mol^{-1} K^{-1}, respectively, with a correlation coefficient of 0.995. The low value of $\Delta H°$ is 6.761 kJ mol^{-1} indicating that the adsorption of fluoride is governed by physisorption process [28,36]. The current work did not show any interaction between parent Amberlite-IRA with F^-, which indicated that no exchange takes place and suggested that Amberlite-IRA-Al is selective to F^-. In other words, F^- was adsorbed to the surface containing Al^{3+}. The low value of $\Delta H°$ indicates that the reaction is not highly affected by changing temperature. Furthermore, the calculated value of $\Delta S°$ was found to be –12.872 J mol^{-1} K^{-1}. The negative values of $\Delta S°$ indicated the increased order and less randomness at the solid solution interface of fluoride with Amberlite-IRA-Al [28].

Table 2
Calculated thermodynamic parameters for the effect of temperature on the adsorption of F^- using Amberlite-IRA-Al

Temperature	Thermodynamic parameters					
	K_L (L mg^{-1})	lnK_L	$\Delta G°$	$\Delta H°$ (kJ mol^{-1})	$\Delta S°$ (J K^{-1} mol^{-1})	R^2
288	0.01263	–4.372	10.468	6.761	–12.872	0.995
293	0.01315	–4.331	10.550			
298	0.01380	–4.283	10.611			
303	0.01433	–4.245	10.694			
308	0.01514	–4.190	10.729			

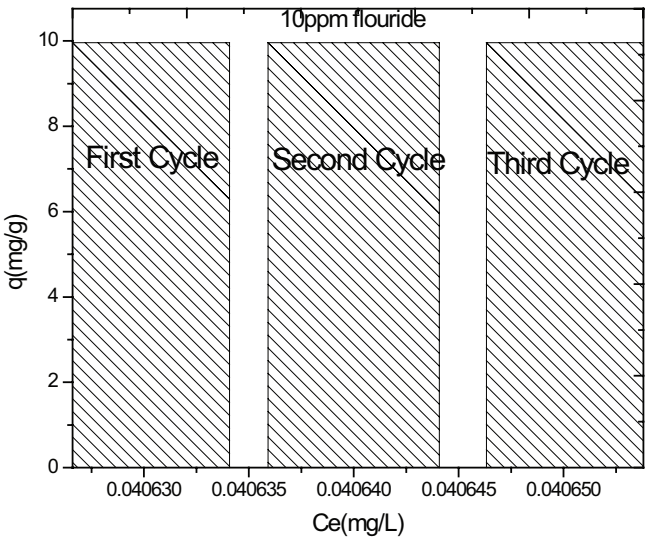

Fig. 9. Successive adsorption cycles for IRA-Al sorbent (experimental conditions: volume 100 mL; absorbent dose 0.1 g; initial concentration 10 mg L^{-1}; and contact time 60 min).

3.7. Desorption isotherm

In order for the adsorption process to be applicable and manageable, the Amberlite-IRA-Al must be easily regenerated. The exhausted sorbent is subjected to a one-step procedure regeneration by adding 2% NaOH to the sorbent. This allows the fluoride ions to be leached out the sorbent. The Amberlite-IRA-Al sorbent is rinsed with distilled water, dried at 50°C–60°C, and then reused [17]. The regenerated Amberlite-IRA-Al sorbent was reused for up to three successive adsorption cycles with the same efficiency. Fig. 9 illustrates that the adsorption capacity of Amberlite-IRA-Al sorbent was not affected after successive cycles. The sorbent can be successfully regenerated and used repeatedly without any loss in its adsorption capacity, which elaborate to its advantages and would economically enhance its application.

3.8. Effect of coexisting ions

Fluoride containing water samples are always accompanied with various common ions. The effect of these coexisting ions on the removal of fluoride was studied as follows.

First, the effect of the competing ion chloride, where a solution of 10 mg L^{-1} chloride was mixed with the 25 mg L^{-1} fluoride solution. The maximum adsorption capacity Q_{max} decreased upon existing of chloride ions. The decrease was observed to be from 24.5 to 17.5 mg g^{-1} (Fig. 10).

Second, the effect of existing of nitrate ions. A solution of 10 mg L^{-1} nitrate ions was mixed with 25 mg L^{-1} solution of fluoride, the maximum capacity of Amberlite-IRA-Al sorbent for fluoride removal decreased from 24.5 to 15 mg g^{-1} (Fig. 10).

The gradual decrease in the fluoride removal in the presence of other common anions may be attributed with the increasing in anionic charge in solution. Interference of multi-anion with fluoride adsorption is probably due to columbic forces [28].

4. Removal of fluoride using fixed-bed column technique

The column experiments aimed to study the effect of various parameters on the adsorption process in fixed-bed column such as inlet flow rate, initial fluoride concentration,

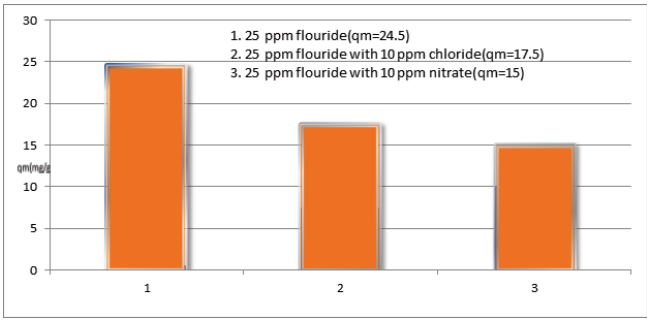

Fig. 10. Removal of 25 ppm fluoride (1) in the absence of competing ions, (2) in the presence of 10 ppm chloride, and (3) in the presence of 10 ppm nitrate.

and bed depth at various throughput volumes. Samples of the outlet bulk solution were collected at definite intervals of time and examined for fluoride concentration. Exhausted Amberlite-IRA-Al bed was regenerated in situ in column via alkali treatment method as done for batch studies.

4.1. The effect of initial fluoride concentration

To investigate the effect of initial concentration of fluoride on the removal process, three runs of different concentrations of fluoride "5.0, 7.5, and 10 mg L^{-1}" were carried out. The results obtained showed that the fluoride uptake increased with decrease in initial concentration [24]. From Fig. 11, breakthroughs of the three concentrations used are 2,839, 2,072, and 1,610 bed volumes, respectively, which is comparable with the same behavior recorded [37].

4.2. The effect of different doses of Amberlite-IRA-Al sorbent

The effect of weight of the new sorbent was studied using 0.25, 0.5, and 1.0 g of Amberlite-IRA-Al. Fig. 12 indicates that the removal of fluoride increased by decreasing the weight of the sorbent. However, we observe that when the number of bed volumes taken into consideration the adsorption process was found to depend on the sorbent depth in the column and not its weight [38]. In other words, the longer the height of the sorbent the larger the number of bed volumes as illustrated in Fig. 12.

4.3. The effect of pH

Fig. 13 shows the effect of pH on removal of fluoride using Amberlite-IRA-Al. Three runs were carried out at pH = 3, 7, and 9. The maximum uptake observed at pH = 3, which was consistent with results obtained in batch experiment.

4.4. The effect of flow rate

The effect of flow rate was also studied. The removal efficiency of fluoride was investigated against different rates (1, 2, and 3 mL min^{-1}). The best breakthrough observed with the flow rate of 3 mL min^{-1} (Fig. 14). This can be explained in terms of surface phenomenon as F^- reach the surface faster it will be adsorbed faster. The maximum uptake recorded at flow rate of 3 mL min^{-1} is similar to that reported before [24].

4.5. Reusing of Amberlite-IRA-Al sorbent after column experiments

Amberlite-IRA-Al sorbent used for the removal of 10 mg L^{-1} fluoride was regenerated with 2% NaOH solution and then reused for another run for the removal of fluoride in 10 ppm solution [17]. Fig. 15 shows the regenerated sorbent exhibited higher efficiency than the original one and this may be attributed to increasing sites of adsorption after adding sodium hydroxide which is already the preparing reagent in

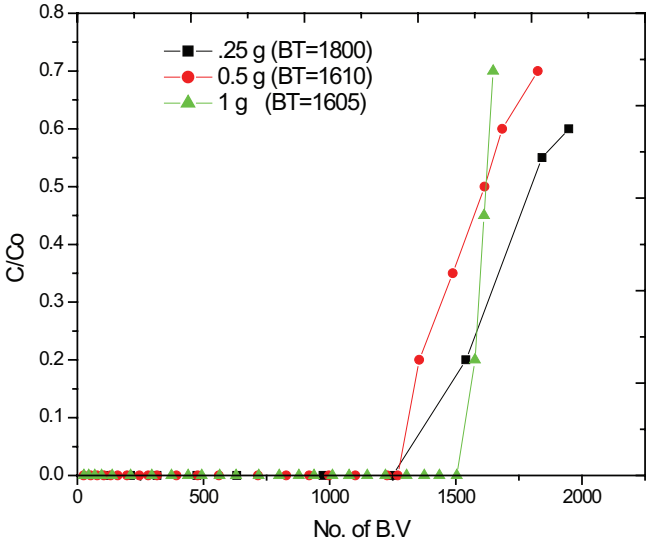

Fig. 12. The effect of using different doses of Amberlite-IRA-Al sorbent on removal process of fluoride.

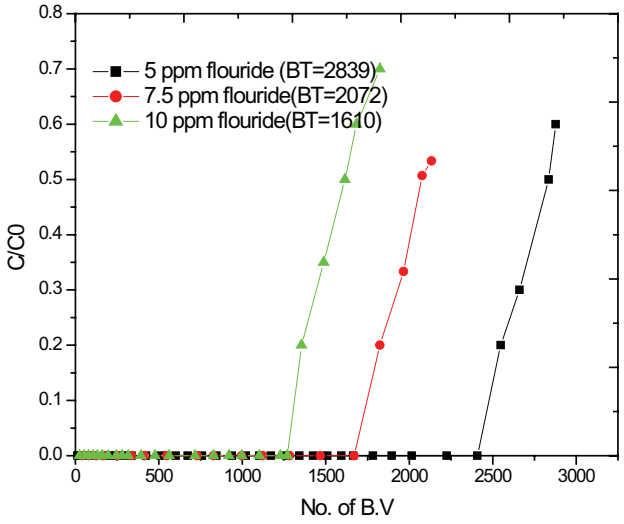

Fig. 11. The effect of initial concentration of fluoride on removal process using IRA-Al sorbent.

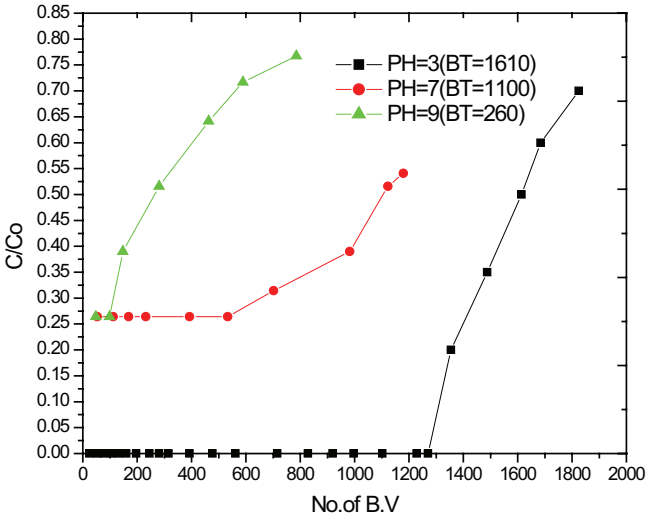

Fig. 13. The effect of pH on removal process of fluoride using Amberlite-IRA-Al sorbent.

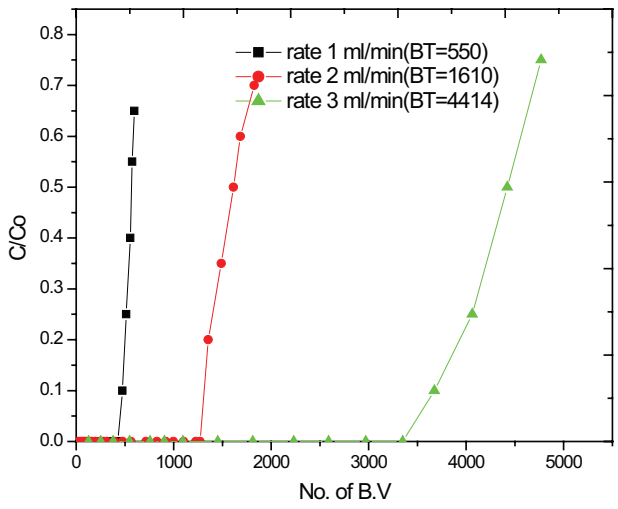

Fig. 14. The effect of flow rate on removal process of fluoride using Amberlite-IRA-Al sorbent.

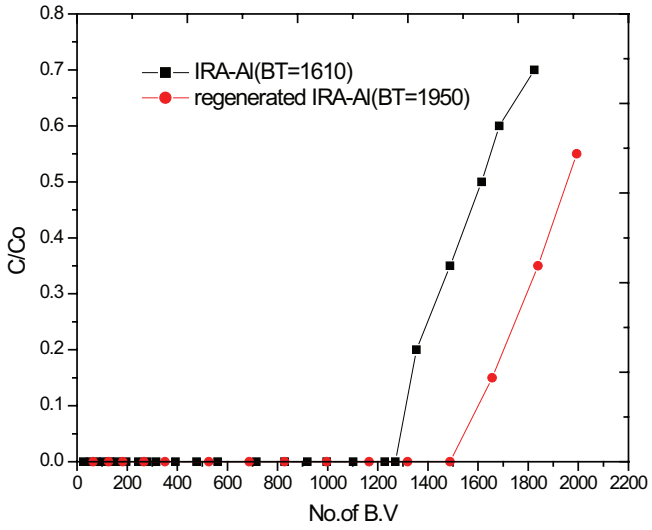

Fig. 15. Reusing of Amberlite-IRA-Al sorbent for two successive runs.

synthesizing the sorbent. This indicates that the Amberlite-IRA-Al is viable and economically preferable as a sorbent and this adds to its advantages as a commercial adsorbent for fluoride.

5. Conclusion

In this study, the novel Amberlite-IRA-Al is prepared and evaluated for the removal of fluoride in both batch and column techniques. It was concluded that it is a suitable adsorbent for the removal of fluoride even in low concentration solutions (5 mg L^{-1}). High adsorption capacities were observed in both batch and column techniques and can be regenerated and reused for successive cycles with efficiency 99% (up to three successive cycles). Batch experiments indicate that the time to attain equilibrium was 8 min and adsorption followed the pseudo-second-order kinetic model. The regression analysis of the equilibrium data fitted the Langmuir isotherm, and the adsorption capacity was 80.33 mg g^{-1}. The defluoridation process strongly depends on the pH of the feed and extensive removal was observed over the range from 3.0 to 7.0. The thermodynamic parameters suggested that the adsorption process with aqueous solutions is governed by physisorption process. The fixed-bed column experiments were analyzed at different flow rates, bed depth, and initial fluoride concentration. The longest breakthrough corresponds to the lowest concentration fed 5 mg L^{-1} and with the highest flow rate applied 3 mL min^{-1}.

Acknowledgments

The authors are grateful to Science Center for Detection & Remediation of Environmental Hazards, Al-Azhar University (SCDREH) for allowing use and conducting most of the measurements of the research in its laboratories.

References

[1] V. Tomar, D. Kumar, A critical study on efficiency of different materials for fluoride removal from aqueous media, Chem. Cent. J., 7 (2013) 51.
[2] X. Fan, D.J. Parker, M.D. Smith, Adsorption kinetics of fluoride on low cost materials, Water Res., 37 (2003) 4929–4937.
[3] P.T.C. Harrison, Fluoride in water: a UK perspective, J. Fluorine Chem., 126 (2005) 1448–1456.
[4] W.B. Apambire, D.R. Boyle, F.A. Michel, Geochemistry, genesis, and health implications of fluoriferous ground waters in the upper regions of Ghana, Environ. Geol., 33 (1997) 13–24.
[5] S. Ghorai, K.K. Pant, Equilibrium, kinetics and breakthrough studies for adsorption of fluoride on activated alumina, Sep. Purif. Technol., 42 (2005) 265–271.
[6] C.Y. Hu, S.L. Lo, W.H. Kuan, Effects of co-existing anions on fluoride removal in electrocoagulation (EC) process using aluminum electrodes, Water Res., 37 (2003) 4513–4523.
[7] R. Sinha, S. Mathur, Control of aluminum in treated water after defluoridation by electrocoagulation and modelling of adsorption isotherms, Desal. Wat. Treat., 57 (2015) 13760–13769.
[8] L. Cumbal, J. Greenleaf, D. Leun, A.K. SenGupta, Polymer supported inorganic nanoparticles: characterization and environmental applications, React. Funct. Polym., 54 (2003) 167–180.
[9] L.M. Blaney, S. Cinar, A.K. SenGupta, Hybrid anion exchanger for trace phosphate removal from water and wastewater, Water Res., 41 (2007) 1603–1613.
[10] A. Genz, A. Kornmuller, M. Jekel, Advanced phosphorus removal from membrane filtrates by adsorption on activated aluminium oxide and granulated ferric hydroxide, Water Res., 38 (2004) 3523–3530.
[11] Y. Zhou, C. Yu, Y. Shan, Adsorption of fluoride from aqueous solution on La^{3+}-impregnated cross-linked gelatin, Sep. Purif. Technol., 36 (2004) 89–94.
[12] S.P. Kamble, S. Jagtap, N.K. Labhsetwar, D. Thakare, S. Godfrey, S. Devotta, S.S. Rayalu, Defluoridation of drinking water using chitin, chitosan and lanthanum-modified chitosan, Chem. Eng. J., 129 (2007) 173–180.
[13] N. Viswanathan, S. Meenakshi, Enhanced fluoride sorption using La(III) incorporated carboxylated chitosan beads, J. Colloid Interface Sci., 322 (2008) 375–383.
[14] X.-H. Wang, R.-H. Song, H.-C. Yang, Y.-J. Shi, G.-B. Dang, S. Yang, Y. Zhao, X.-F. Sun, S.-G. Wang, Fluoride adsorption on carboxylated aerobic granules containing Ce(III), Bioresour. Technol., 127 (2013) 106–111.
[15] V. Ganvir, K. Das, Removal of fluoride from drinking water using aluminum hydroxide coated rice husk ash, J. Hazard. Mater., 185 (2011) 1287–1294.

[16] Y. Zhao, X. Li, L. Liu, F. Chen, Fluoride removal by Fe(III)-loaded ligand exchange cotton cellulose adsorbent from drinking water, Carbohydr. Polym., 72 (2008) 144–150.
[17] M.J. DeMarco, A.K. SenGupta, J.E. Greenleaf, Arsenic removal using a polymeric/inorganic hybrid sorbent, Water Res., 37 (2003) 164–176.
[18] Q. Zhang, B. Pan, X. Chen, W. Zhang, B. Pan, Q. Zhang, L. Lv, X.S. Zhao, Preparation of polymer-supported hydrated ferric oxide based on Donnan membrane effect and its application for arsenic removal, Sci. China, Ser. B, 51 (2008) 379–385.
[19] M.A. Faraj-Zadeh, E.G. Kalhor, Extraction–spectrophotometric method for determination of fluoride in the range of microgram per liter in natural waters, Microchim. Acta, 137 (2001) 169–171.
[20] J.A. Arancibia, A. Rullo, A.C. Olivieri, S.D. Nezio, M. Pistonesi, A. Lista, B.S.F. Band, Fast spectrophotometric determination of fluoride in ground waters by flow injection using partial least-squares calibration, Anal. Chim. Acta, 512 (2004) 157–163.
[21] A.K. Sengupta, L. Lim, Modeling chromate ion-exchange processes, AIChE J., 34 (1988) 2019–2029.
[22] W.D. Henry, D. Zhao, A.K. SenGupta, C. Lange, Preparation and characterization of a new class of polymeric ligand exchangers for selective removal of trace contaminants from water, React. Funct. Polym., 60 (2004) 109–120.
[23] S. Zhang, Y. Lu, X. Lin, X. Su, Y. Zhang, Removal of fluoride from groundwater by adsorption onto La(III)–Al(III) loaded scoria adsorbent, Appl. Surf. Sci., 303 (2014) 1–5.
[24] N. Chen, Z. Zhang, C. Feng, M. Li, R. Chen, N. Sugiura, Investigations on the batch and fixed-bed column performance of fluoride adsorption by Kanuma mud, Desalination, 268 (2011) 76–82.
[25] A. Bhatnagar, E. Kumar, M. Sillanpää, Fluoride removal from water by adsorption—a review, Chem. Eng. J., 171 (2011) 811–840.
[26] H. Basu, R.K. Singhal, M.V. Pimple, A.V.R. Reddy, Synthesis and characterization of alumina impregnated alginate beads for fluoride removal from potable water, Water Air Soil Pollut., 224 (2013) 1572.
[27] P. Praipipat, M.M. El-Moselhy, K. Khuanmar, P. Weerayutsil, T.T. Nguyen, S. Padungthon, Enhanced defluoridation using reusable strong acid cation exchangers in Al^{3+} form (SAC-Al) containing hydrated Al(III) oxide nanoparticles, Chem. Eng. J., 314 (2017) 192–201.
[28] H. Kaygusuz, S. Uzaşçı, F.B. Erim, Removal of fluoride from aqueous solution using aluminum alginate beads, CLEAN – Soil Air Water, 43 (2015) 724–730.
[29] A. Tor, N. Danaoglu, G. Arslan, Y. Cengeloglu, Removal of fluoride from water by using granular red mud: batch and column studies, J. Hazard. Mater., 164 (2009) 271–278.
[30] W.-X. Gong, J.-H. Qu, R.-P. Liu, H.-C. Lan, Adsorption of fluoride onto different types of aluminas, Chem. Eng. J., 189–190 (2012) 126–133.
[31] S.-G. Wang, Y. Ma, Y.-J. Shi, W.-X. Gong, Defluoridation performance and mechanism of nano-scale aluminum oxide hydroxide in aqueous solution, J. Chem. Technol. Biotechnol., 84 (2009) 1043–1050.
[32] X.-j. Hu, J.-s. Wang, Y.-g. Liu, X. Li, G.-m. Zeng, Z.-l. Bao, X.-x. Zeng, A.-w. Chen, F. Long, Adsorption of chromium (VI) by ethylenediamine-modified cross-linked magnetic chitosan resin: isotherms, kinetics and thermodynamics, J. Hazard. Mater., 185 (2011) 306–314.
[33] S. Gueu, B. Yao, K. Adouby, G. Ado, Kinetics and thermodynamics study of lead adsorption on to activated carbons from coconut and seed hull of the palm tree, Int. J. Environ. Sci. Technol., 4 (2007) 11–17.
[34] S. Hena, Removal of chromium hexavalent ion from aqueous solutions using biopolymer chitosan coated with poly 3-methyl thiophene polymer, J. Hazard. Mater., 181 (2010) 474–479.
[35] M. Roulia, A.A. Vassiliadis, Sorption characterization of a cationic dye retained by clays and perlite, Microporous Mesoporous Mater., 116 (2008) 732–740.
[36] M. Kara, H. Yuzer, E. Sabah, M.S. Celik, Adsorption of cobalt from aqueous solutions onto sepiolite, Water Res., 37 (2003) 224–232.
[37] A. Teutli-Sequeira, M. Solache-Ríos, V. Martínez-Miranda, I. Linares-Hernández, Behavior of fluoride removal by aluminum modified zeolitic tuff and hematite in column systems and the thermodynamic parameters of the process, Water Air Soil Pollut., 226 (2015) 239.
[38] P.B. Bhakat, A.K. Gupta, S. Ayoob, Feasibility analysis of As(III) removal in a continuous flow fixed bed system by modified calcined bauxite (MCB), J. Hazard. Mater., 139 (2007) 286–292.

Supplementary materials

To calculate the breakthrough we make use of the following equation:

Bed volume (B.V.) = (π) (r^2) (h)

where r = is the radius of column (5.5 mm); h = is the height of exchanger in the column.

Also the number of bed volumes can be calculated as follows:

$$\text{No. of B.V} = \frac{\text{volume of water passed x flow rate}}{\text{B.V.}}$$

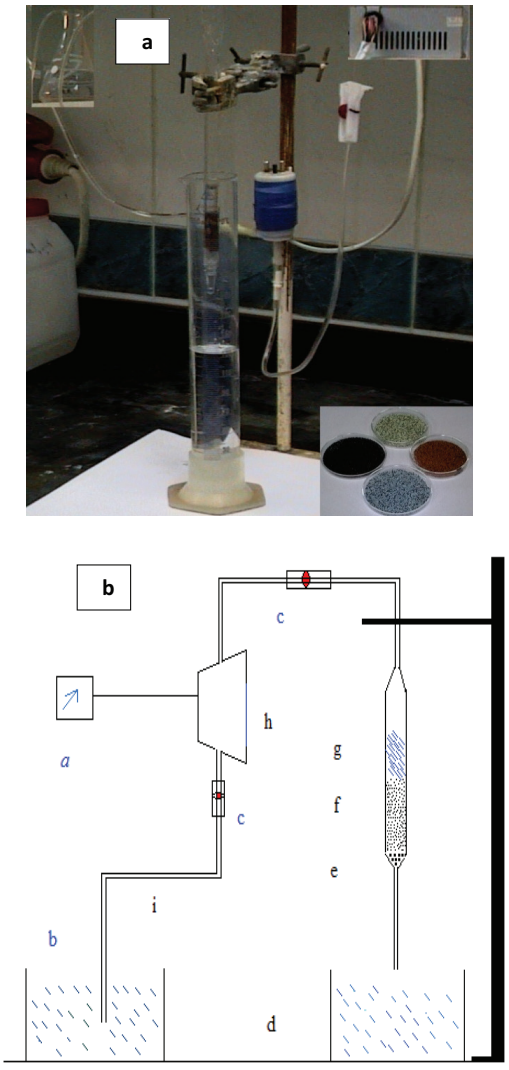

Fig. S1. (a) Constructed system, (b) schematic diagram of the set up used in treatment is as follows: *a*, power supply (9 V); *b*, influent; *c*, input and output valves; *d*, effluent; *e*, glass wool; *f*, exchanger beads; *g*, contact liquid; and *h*, water pump.

All experimental data are plotted in figures between the concentration ratio (C/C_o) of the pollutant under investigation, where C_o is the starting concentration before passing through bed and C is its concentration after passing through bed at varies intervals. This ratio is plotted on the y-coordinate against the no. of B.V. as x-coordinate. The breakthrough reached when half of the initial concentration appears in the effluent solution.

Table S1
Parameters obtained from pseudo-first-order

Concentration (mg L^{-1})	K_1 (min^{-1})	R^2
25	0.056	0.722
50	0.118	0.757
75	0.119	0.870
100	0.122	0.857

Table S2
Parameters obtained from pseudo-second-order

Concentration (mg L^{-1})	K_2 (g mg^{-1} min^{-1})	R^2
25	0.167	0.9999
50	0.131	0.9999
75	0.058	0.9999
100	0.028	0.9999

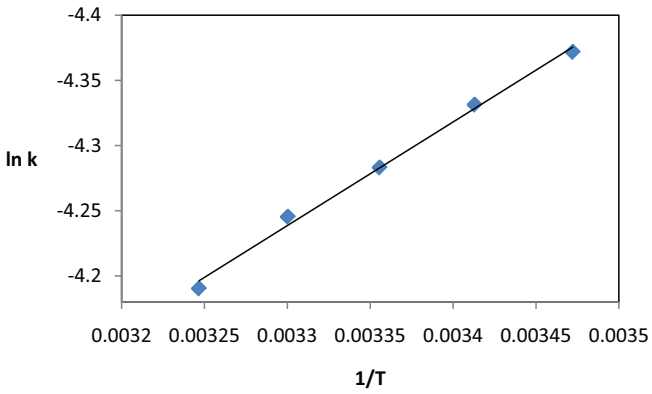

Fig. S2. Plot of ln$K$ vs. 1/T for the adsorption process using Amberlite-IRA-Al sorbent.